On the Direct Numerical Simulation of moderate-Stokes-number turbulent particulate flows using Algebraic-Closure-Based and Kinetic-Based Moment Methods

By A. Vié†‡, E. Masi ¶, O. Simonin ¶ AND M. Massot†‡

In turbulent particulate flows, the occurrence of particle trajectory crossings (PTC) is the main constraint on classical monokinetic Eulerian methods. To handle such PTC, accounting for high-order moments of the particle velocity distribution is mandatory. In the simplest case, second-order moments are needed. To retrieve these moments, two solutions are proposed in the literature: the Algebraic-Closure-Based Moment Method (ACBMM) and the Kinetic-Based Moment Method (KBMM). The ACBMM provides constitutive relations for the random-uncorrelated-motion (RUM) particle kinetic stress tensor as algebraic closures based on physical arguments (Simonin *et al.* 2002; Kaufmann *et al.* 2008; Masi 2010; Masi & Simonin 2012). These closures rely on the internal energy, namely the RUM particle kinetic energy, which is obtained using an additional transport equation. Alternatively, it is possible to directly solve for the second-order moment by providing a closure for the third-order correlation. The KBMM proposes a kinetic description, that is, the number density function (NDF) is reconstructed based on the resolved moments and on a presumed shape. In the present work, an isotropic Gaussian and the anisotropic Gaussian closure of Vié *et al.* (2012) are used. The goal of the present study is to provide a first comparison between ACBMM and KBMM, using the same robust numerical methods, in order to highlight differences and common points. The test case is a 2D turbulent flow with a mean shear, which is designed in order to mimic the injection of particles into a turbulent gas field.

1. Introduction

Particle-laden turbulent flows occur in several industrial applications (automotive engines, gas turbines, fluidized beds, etc.). In order to simulate these flows, both Eulerian and Lagrangian methods may be used. Eulerian methods are preferred because of their intrinsic abilities for high-performance computing (HPC), ease of coupling with the gas phase due to the Eulerian representation of the disperse phase, and statistical convergence. However, particular attention should be focused on the modeling and numerical methods. Indeed, solving for the moments implies a loss of information, and the primary goal of the Eulerian modeling should be to recover this lack. Furthermore, as the result-

† CNRS, UPR 288, Laboratoire d'Energétique moléculaire et macroscopique, combustion, Grande Voie des Vignes, 92295 Chatenay-Malabry, France
‡ Ecole Centrale Paris, Grande Voie des Vignes, 92295 Chatenay-Malabry, France
¶ CNRS, UMR 5502 , Institut de Mécanique des Fluides de Toulouse, 2 Allée du Professeur Camille Soula, 31400 Toulouse, France

ing system of equations is hyperbolic or weakly hyperbolic, dedicated numerical methods may be needed.

In the literature, several models based on different assumptions have been suggested. They can be split into two categories, one dealing with Stokes numbers smaller than the critical one ($\mathrm{St}_K < 1$ based on the Kolmogorov time scale), the other recovering a larger range of Stokes numbers, higher than the critical one. In the first category, the simplest model in terms of number of transported moments is the fast Eulerian method of Ferry & Balachandar (2001). This model only solves for the particle number density, whereas the velocity of the disperse phase is expressed as a function of the gas velocity by means of a Taylor expansion of the particle velocity. In solving for an additional equation of the momentum, two models exist: the multifluid approach of Laurent & Massot (2001) and Freret *et al.* (2012), which assumes a monokinetic description of the particle velocity, and the two-fluid model of Druzhinin & Elghobashi (1998), which uses a volume average instead of an ensemble average. Such models are limited by the fact that they consider only one averaged velocity, and thus are unable to capture PTC which involve several velocities in the same volume of control.

To handle PTC in dilute particle-laden turbulent flows in the framework of the direct numerical simulation (DNS), Février *et al.* (2005) suggested a conditional statistical approach. It relies on the partitioning of the particle velocity into a spatially correlated field, shared by all the particles, and a random-uncorrelated-motion (RUM) contribution, proper to each particle. According to this approach, moment equations can be derived from the conditional NDF. The resulting system of equations is unclosed because of the unknown RUM particle kinetic stress tensor appearing in the flux term of the momentum equation (which is, in fact, a central second-order moment). To close this term, two strategies are proposed in the literature: the Algebraic-Closure-Based Moment Method (ACBMM) and the Kinetic-Based Moment Method (KBMM).

The ACBMM closes the RUM stress tensor by providing constitutive relations based on physical and/or mathematical arguments, using a supplementary equation for the RUM kinetic energy. The simplest closure was proposed by Simonin *et al.* (2002), Kaufmann *et al.* (2008), and it is based on a viscosity-like assumption. More recently, Masi (2010) derived more complex closures, suggesting the explicit algebraic stress model 2Φ-EASM (Masi & Simonin 2012) as the most accurate. This model uses an assumption of self-similarity of the RUM stress tensor, similar to the assumption of "weak-equilibrium" used in turbulence for closing the Reynolds stresses (So *et al.* 2004). The ACBMM has been implemented in the AVBP code and tested on several academic and industrial applications, with the same results: the viscosity closure may be successfully used in homogeneous isotropic turbulence (Kaufmann *et al.* 2008) whereas it fails in mean sheared flows. Preliminary Eulerian simulations showed that this model drastically overestimate the dissipation rate of the disperse phase (Riber 2007) and that the alternative 2Φ-EASM is preferable (Sierra 2012).

The KBMM, instead of closing the RUM stress tensor by physical/mathematical arguments, suggests directly solving for each of its components. The strategy relies on a presumed NDF shape which has as many parameters as the number of moments we want to describe. Several kinetic closures exist (Massot *et al.* 2004; Kah *et al.* 2010; Yuan & Fox 2011; Vié *et al.* 2011, 2012), the choice of which depends on accuracy requirements, as well as on computational costs. Compared to the ACBMM, the KBMM is more expensive for the same level of modeling (second-order moment closures) as it solves for all the components of the tensor. The former is indeed a first-order modeling, whereas

the latter is a second-order one. Nevertheless, the KBMM has the major advantage of having a well-defined mathematical structure of the resulting system of equations, which can be solved using identified and well-defined hyperbolic solvers.

In the present work, the ACBMM and the KBMM are compared through two closures for each: (i) the viscosity-like assumption (referred to as VISCO) and the 2Φ-EASM for the ACBMM; (ii) the isotropic and anisotropic Gaussian closures for the KBMM. The test case is a 2D isothermal homogeneous isotropic turbulence with a mean shear; it has been designed to mimic the injection of particles into a turbulent gas field, directly inspired by the 3D case proposed by Vermorel *et al.* (2003) and more recently studied in Masi (2010), Dombard (2011), and Sierra (2012). It provides the groundwork for a more intensive study that will investigate modeling issues in conjunction with the development of adapted numerical methods for 3D simulations.

2. Modeling

2.1. *The conditional statistical approach and the moment equations*

In order to define the particle velocity distribution for a disperse phase experiencing the PTC phenomenon, a conditional statistical approach is used (Simonin *et al.* 2002; Février *et al.* 2005). It relies on a conditional probability density function on one given fluid flow realization $\mathscr{H}_f$, the moments of which describe the disperse phase in a Eulerian framework. The zero order moment is the particle number density $\tilde{n}_p$; the first-order moment is the conditional ensemble-averaged particle velocity $\tilde{\mathbf{u}}_p(\mathbf{x},t) = < \mathbf{u}_p(t)|\mathbf{x}_p(t)=\mathbf{x};\mathscr{H}_f >$. Second-order and third-order central order moments are defined, respectively, as $R_{p,ij}(\mathbf{x},t) = \langle \delta u_{p,i}(t)\delta u_{p,j}(t)|\mathbf{x}_p(t)=\mathbf{x};\mathscr{H}_f\rangle$ and $Q_{p,ijk}(\mathbf{x},t) = \langle \delta u_{p,i}(t)\delta u_{p,j}(t)\delta u_{p,k}(t)|\mathbf{x}_p(t)=\mathbf{x};\mathscr{H}_f\rangle$, where $\delta u_{p,i}(t) = u_{p,i}(t) - \widetilde{u}_{p,i}(\mathbf{x}_p(t),t)$ is the RUM particle velocity as modeled by the MEF velocity decomposition (Février *et al.* 2005), accounting for the chaotic particles' behavior. The first-order moment together with high-order RUM moments ensure a unique particle velocity distribution. Hereafter, the tilde symbol over $\tilde{n}_p$ and $\tilde{\mathbf{u}}_p$ is dropped.

In the framework of the moment approach, the transport equations for the particle Eulerian moments are obtained by analogy with the kinetic theory of dilute gases, integrating the moments of the NDF over the particle velocity space. In isothermal conditions, zero and first-order moment equations are

$$\frac{\partial n_p}{\partial t} + \frac{\partial n_p u_{p,m}}{\partial x_m} = 0 \tag{2.1}$$

$$\frac{\partial n_p u_{p,i}}{\partial t} + \frac{\partial n_p (u_{p,i}u_{p,m} + R_{p,im})}{\partial x_m} = -n_p \frac{u_{p,i} - u_{g,i}}{\tau_p} \tag{2.2}$$

In order to use the system (2.2), a closure for the second-order RUM velocity correlations, i.e., the particle kinetic RUM stress tensor $R_{p,ij}$ must be provided.

2.2. *The algebraic closure-based moment method*

The ACBMM closes the RUM stresses by physical/mathematical assumptions on their evolution. Decomposing the RUM stress tensor in deviatoric and isotropic parts $R_{p,ij} = R^*_{p,ij} + P\delta_{ij}$, where $P = R_{p,kk}/N_{dim} = 2\delta\Theta_p/N_{dim}$ is the pressure and $\delta\Theta_p$ is the RUM kinetic energy (RUE), the ACBMM solves the RUE by an additional transport equation while providing algebraic closures for the deviatoric part of the RUM stress tensor. In Masi (2010), a hierarchy of closures has been suggested, and here we focus on two of them:

a viscosity-like assumption (Simonin *et al.* 2002; Kaufmann *et al.* 2008), referred to as the VISCO model, and the 2Φ-EASM (Masi & Simonin 2012), a non-linear algebraic closure already evaluated in preliminary Eulerian-Eulerian simulations of particle-laden mean sheared flows (Sierra 2012). The model VISCO uses a local equilibrium assumption on the components of the stress tensor in conjunction with an assumption of light anisotropy, and reads

$$\mathbf{R}_p^* = -2\nu\mathbf{S}^*, \tag{2.3}$$

where $\nu = \tau_p\delta\Theta_p/N_{dim}$ and $S_{ij}^* = S_{ij} - 1/N_{dim}S_{kk}\delta_{ij}$ with $S_{ij} = 1/2(\partial_{x_j}u_{p,i} + \partial_{x_i}u_{p,j})$. The 2Φ-EASM relies on a hypothesis of self-similarity of the tensor, which leads to the implicit model for the particle RUM anisotropy $\mathbf{b}^* = \mathbf{R}_\mathbf{p}^*/2\delta\Theta_p$

$$\mathbf{b}^*\left(-2\{\mathbf{b}^*\mathbf{S}^*\}\right) = -\frac{2}{N_{dim}}\mathbf{S}^* + (\mathbf{b}^*\mathbf{\Omega} - \mathbf{\Omega}\mathbf{b}^*) - (\mathbf{b}^*\mathbf{S}^* + \mathbf{S}^*\mathbf{b}^* - \frac{2}{N_{dim}}\{\mathbf{b}^*\mathbf{S}^*\}\mathbf{I}), \tag{2.4}$$

where curly brackets stand for the tensor trace. Eq. (2.4) is made explicit using techniques well known in turbulence (Girimaji 1996). An explicit solution is given as follows:

$$\mathbf{b}^* = G_1\mathbf{S}^* + G_2\left(\mathbf{S}^*\mathbf{\Omega} - \mathbf{\Omega}\mathbf{S}^*\right) + G_3(\mathbf{S}^{*2} - \frac{1}{N_{dim}}\left\{\mathbf{S}^{*2}\right\}\mathbf{I}) \tag{2.5}$$

where $\Omega_{ij} = 1/2(\partial_{x_j}u_{p,i} - \partial_{x_i}u_{p,j})$ is the particle vorticity tensor. In 2D configurations, only the first two tensors in Eq. (2.5) form an integrity basis and only two coefficients are thus needed for the explicit solution. They are modeled using the particle rate-of-strain and particle vorticity second invariants, $\eta_1 = \left\{\mathbf{S}^{*2}\right\}$ and $\eta_2 = \left\{\mathbf{\Omega}^2\right\}$, as $G_2 = -1/2\eta_1$ and $G_1 = -\sqrt{2\eta_1 + 2\eta_2}/2\eta_1$, where the most probable sign is retained. In this work, the contracted third-order correlation appearing into the RUE equation is neglected.

2.3. *The kinetic-based moment method*

Instead of using constitutive relationships for the second-order moment, one may directly transport all its components. At this point a further closure problem arises, as third-order correlations are unknown. This concern may be addressed by using the KBMM. By this strategy, a presumed shape for the NDF needs to be provided, with as many parameters as the number of transported moments. Several closures exist in the literature (Laurent & Massot 2001; Massot *et al.* 2004; Yuan & Fox 2011; Vié *et al.* 2011, 2012) that make it possible to account for trajectory crossings with an increasing complexity. Here we use the anisotropic Gaussian closure (Vié *et al.* 2012), inspired by Levermore & Morokoff (1996), as it represents the simplest shape verifying the second-order moments

$$f_G(t,x,\mathbf{c}_p) = \frac{n_p}{2\pi\sqrt{|\mathbf{R}_p|}}\exp\left(-(\mathbf{c}_p - \mathbf{u}_p)^T\mathbf{R}_p^{-1}(\mathbf{c}_p - \mathbf{u}_p)\right). \tag{2.6}$$

The Gaussian closure has 6 parameters in 2D flows: n_p, $\mathbf{u}_p$ and $\mathbf{R}_p$, which are the transported quantities. Instead of transporting $\mathbf{R}_p$, which are central moments and lead to non-conservative terms, the full second-order moments $E_{ij} = n_p(u_{p,i}u_{p,j} + R_{p,ij})$ are solved

$$\frac{\partial n_pE_{ij}}{\partial t} + \frac{\partial n_p\left(E_{ij}u_{p,m} + u_{p,i}R_{p,jm} + u_{p,j}R_{p,im}\right)}{\partial x_m} = -\frac{n_p}{\tau_p}\left(2E_{ij} - u_{g,i}u_{p,j} - u_{g,j}u_{p,i}\right). \tag{2.7}$$

The interest of the KBMM using the Gaussian closure is that we obtain an hyperbolic system of equations with source terms. This system is mathematically well defined, contrary to that of the ACBMM. However, the main drawback is that one needs to transport

more moments than the ACBMM (in 2D, 4 components for the ACBMM and 6 for the KBMM, and in 3D, 5 for the ACBMM and 10 for the KBMM).

In the following, two types of Gaussian closures are used: the anisotropic Gaussian closure (ANISO) which uses all the components of the second-order moment, and the isotropic Gaussian closure (ISO) which uses only the RUE. The ISO closure is used as a comparison to highlight the importance of the off-diagonal components of the RUM, as ISO corresponds to the ACBMM closed with only the tensor trace.

3. Numerical methods

In terms of numerical methods, the ACBMM and the KBMM require three types of terms to be solved: the hyperbolic and source terms, which exist in both ACBMM and KBMM, and the fluxes of the deviatoric tensor, which need to be solved separately as they are not expected to be hyperbolic. Here the novelty of our approach is that the full system of equations is split into these three terms. This way allows a fully realizable method to be designed, as we need to ensure the realizability of separated blocks instead of the whole system.

The first solver concerns the hyperbolic part of the moment equations. For the KBMM, the fluxes contain the full second-order moment, whereas they contain only the mean and the isotropic part of the fluxes for ACBMM. To solve this system of equations, a second order MUSCL/HLL scheme is used (van Leer 1979), which uses four ingredients :

(a) a dimensional splitting: each direction is solved alternatively,
(b) a linear reconstruction of the primitive variable n_p, $u_{p,i}$, $R_{p,ij}$ (Vié *et al.* 2012),
(c) a flux evaluation at each interface using an HLL scheme,
(d) a temporal update using a two-step Runge-Kutta method.

The resulting scheme is second-order accurate in space and time, and ensures the realizability of the moments, thanks to the reconstruction strategy on the primitive variables (Vié *et al.* 2012), which is not obvious for classical schemes.

The source terms are evaluated using an exact integration considering a constant gas velocity during the time step. This algorithm is unconditionally stable, and preserves the moment space.

The tensor $R_{p,ij}$ evaluated by the ACBMM may have a diffusive structure for VISCO, but is more complex for 2Φ-EASM. For a diffusive operator, the stability condition for a central scheme for the second-order derivative is well defined, but such a condition for the 2Φ-EASM needs to be defined. Actually, we keep a classical second-order central scheme for VISCO as well as for 2Φ-EASM, evaluated in two steps:

(a) first, the tensors $S_{p,ij}$ and $\Omega_{p,ij}$ are evaluated using a centered scheme,
(b) then, the fluxes of $R_{p,ij}$ are evaluated again using a centered scheme.

Finally, this algorithm uses a 5-cell stencil, and is second-order accurate. For VISCO, the stability condition is the Fourier condition for diffusive equations ($\nu\Delta t/\Delta x^2 < 0.5$). The same stability condition is pragmatically kept for 2Φ-EASM. Note that a mathematical analysis of its structure would be needed but that is beyond the scope of this proceeding. For both the closures VISCO and 2Φ-EASM, realizability conditions based on the Schwarz's inequality and the positiveness of the RUE (Schumann 1977) are imposed.

4. Test case

In order to assess the models, a 2D case similar to the 3D case investigated in Masi & Simonin (2012) was chosen; this configuration mimics the injection of particles in a

turbulent flow. The size of the domain is $L_{box} = 2\pi$ and the mesh is composed of 256^2 cells. The gas field consists of a hyperbolic-tangent gas velocity (the jet) supplemented with a decaying homogeneous isotropic turbulence $\mathbf{u}_g(t=0) = \mathbf{u}_g^{Jet} + \mathbf{u}_g^{HIT}$ with

$$u_{g,1}^{Jet} = \frac{u_0}{2}\left(\tanh\left(\frac{y+\delta_1}{\delta_2}\right) - \tanh\left(\frac{y-\delta_1}{\delta_2}\right)\right), \quad u_{g,2}^{Jet} = 0, \tag{4.1}$$

where $u_0 = 0.1m/s$, $\delta_1 = 0.75m$ and $\delta_2 = 0.066m$. The statistical properties of $\mathbf{u}_g^{HIT}$ are as follows: total kinetic energy=$10^{-4}m^2/s^2$, total dissipation rate=$1.77\times10^{-4}m^2/s^3$, Kolmogorov time scale $\tau_K = 6.03s$ and length scale $l_K = 1.97\times10^{-2}m$, and integral length scale $L_{11} = 0.2m$.

Particles are injected uniformly inside the jet ($n_p(x,y) = 1$ if $x \in [\pi - \delta_1/2, \pi + \delta_1/2]$, $n_p(x,y) = 0$ otherwise), at the same velocity as the gas ($\mathbf{u}_{p,i} = \mathbf{u}_{g,i}$).

Four test cases were analyzed, each differing by the particle Stokes number ($\mathrm{St}_K = 0.1, 1, 5, 10$) which was defined over the initial Kolmogorov time scale as $\mathrm{St}_K = \tau_p/\tau_{K(t=0)}$.

For each Stokes number, a computation of reference was carried out using a Lagrangian Discrete Particle Simulation with 10 million particles. The solver is based on an exact integration of the particle trajectory ODE assuming a constant gas phase velocity during the time step. Moments of the Lagrangian simulations are computed using a box filter of size Δx, i.e., the moments of each cell are obtained by gathering the individual contribution of each particle inside the cell.

5. Results

In Figure 1, visualizations of the particle number density for each model and Stokes number are shown. Results show that all the models give a similar prediction on the instantaneous particle number density for the simulation corresponding to the smallest Stokes number $\mathrm{St}_K = 0.1$. These results were expected as PTC do not occur for low-enough particle inertia; as a consequence, accounting for a velocity dispersion seems to have no impact on the low-order moment predictions. Similar conclusions apply to the numerical simulations corresponding to a particle Stokes number of about unity. However, in this case Eulerian results look more diffused when compared to the Lagrangian predictions, suggesting that a finer mesh would be necessary in order to capture the finer structures occurring in such a highest-preferential-concentration configuration.

Corresponding to higher Stokes number simulations ($\mathrm{St}_K = 5, 10$), Lagrangian results show complex structures composed of crossing thin filaments. For such particle inertia, PTC occur and significant differences between the models may be pointed out. Indeed, results show that the models ANISO and 2Φ-EASM significantly increase with the Stokes number the accuracy of the predictions if compared to the models ISO and VISCO. It is conjectured that an isotropic assumption (ISO) is not adequate for reproducing the effects of PTC which are, by their nature, strongly anisotropic. For the same reason, a model based on a light-anisotropy assumption (VISCO) would be inadequate (Masi *et al.* 2010). For even larger Stokes numbers one can expect that no model would be able to predict the small-scale structures. This limitation is mainly due to the fact that such structures are generated by large-scale trajectory crossings that cannot be captured by pressure-like models, because higher-order moments are needed (Vié *et al.* 2011).

In order to give a quantitative insight, in Figure 2 spatial-averaged results about the RUM stress tensor (deviatoric part and RUE) and the particle number density are depicted. Results show that for low particle inertia ($\mathrm{St}_K \leq 1$) models give similar results;

the main difference appears on the cross-streamwise component of the RUM deviatoric tensor which has a negligible influence in that case, as the total amount of the RUM kinetic energy is well predicted. Note also that for $\mathrm{St}_K = 1$ the mean number density is well reproduced despite the corresponding instantaneous values. For large Stokes numbers ($\mathrm{St}_K = 5, 10$), ISO is found to underestimate the level of the RUE in constrast to VISCO which tends to overestimate the total amount. This model experiences another limit which directly stems from the assumption of equilibrium applying to the components of the stress tensor. This model uses the particle response time as the time scale; it was shown that such a time scale is not appropriate for modeling the evolution of the RUM stresses (Masi 2010), leading to overestimate the cross-to-streamwise component and an underestimate of the amount of the streamwise component. Satisfactory results are instead provided by the models ANISO et 2Φ-EASM which need to account for the anisotropy effect in the modeling. Finally, Lagrangian results exhibit a dissymmetry that is underestimated by Eulerian methods.

6. Conclusions

The two approaches KBMM and ACBMM were compared using two different closures of each. As a test case, a 2D temporal planar jet consisting in a mean shear superposed to a homogeneous isotropic turbulence was used. Results showed that for low particle inertia ($\mathrm{St}_K \leq 1$) all the models and their respective closures give similar results and a good agreement with the Lagrangian data. As the particle inertia increases, the anisotropy has to be accounted for. As a consequence, only the closures ANISO and 2Φ-EASM of the respective approaches KBMM and ACBMM are found to correctly predict the disperse phase at high Stokes numbers. The two strategies, KBMM and ACBMM, showed similar results about the predictions of low- and high-order moments. However, a higher level of accuracy of the model KBMM using ANISO was observed. This result was expected as this model is a second-order modeling which directly solves for the components of the stress tensor, whereas the ACBMM closes them using 2Φ-EASM. To provide perspective, a further comparison between ANISO and 2Φ-EASM is needed in a 3D case, as well as third-order closures for ACBMM. Moreover, to provide more accurate numerical methods, a further investigation of the mathematical behavior of each strategies is envisaged.

Acknowledgments

The authors would like to thank the SAFRAN group, which sponsored the stay of Aymeric Vié, as well as the CTR for the technical support during the Summer Program 2012. The support of the France-Stanford Center for Interdisciplinary Studies through a collaborative project grant (P. Moin/M. Massot) is also gratefully acknowledged.

REFERENCES

Dombard, J. 2011 Direct Numerical Simulation of non-isothermal dilute sprays using the Mesoscopic Eulerian Formalism. PhD thesis, INP Toulouse.

Druzhinin, O. & Elghobashi, S. 1998 Direct numerical simulations of bubble-laden turbulent flows using the two-fluid formulation. *Phys. Fluids* **10**, 685–697.

Ferry, J. & Balachandar, S. 2001 A fast Eulerian method for disperse two-phase flow. *Int. J. Multiphase Flow* **27**, 1199–1226.

Février, P., Simonin, O. & Squires, K. D. 2005 Partitioning of particle velocities in

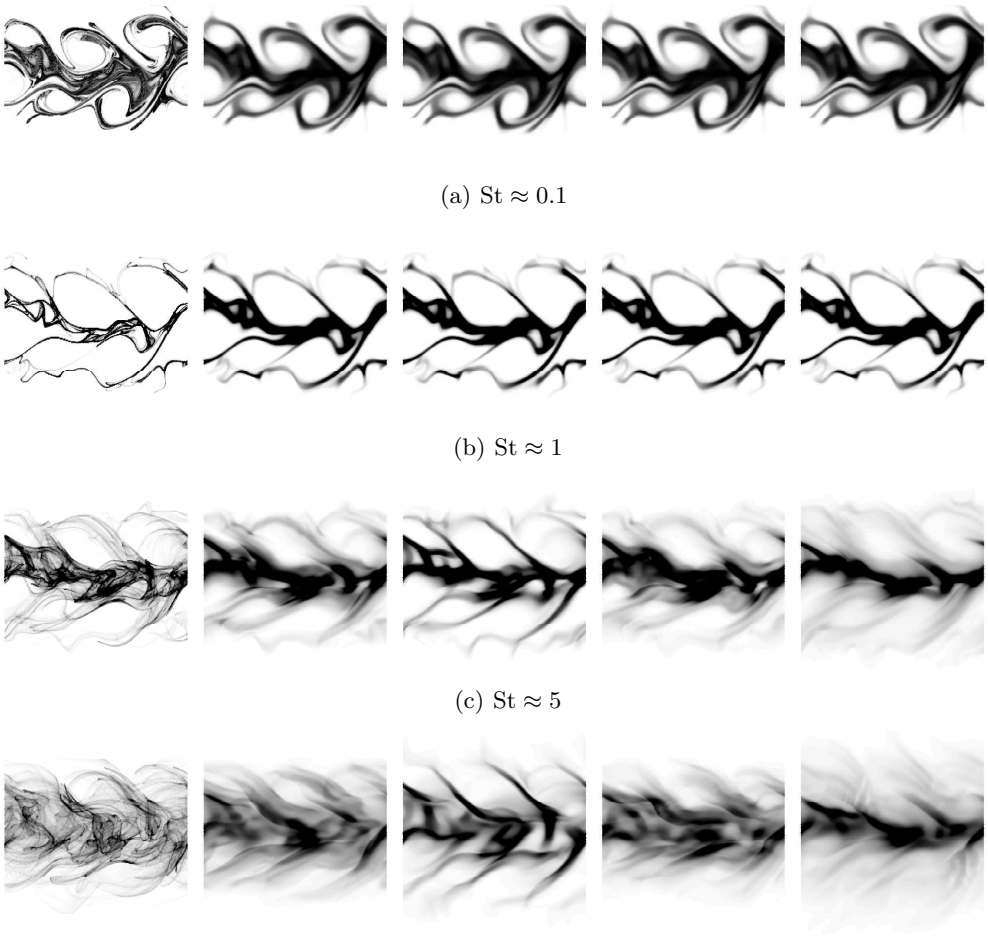

(a) St ≈ 0.1

(b) St ≈ 1

(c) St ≈ 5

(d) St ≈ 10

FIGURE 1. Snapshots of the particle number density, at the time $t = 105s$. St ≈ 0.1 (a), St ≈ 1 (b), St ≈ 5 (c), St ≈ 10 (d). From left to right: Eulerian-Lagrangian DNS, Eulerian-Eulerian DNS using anisotropic Gaussian, isotropic Gaussian, 2Φ-EASM and viscosity algebraic closures.

gas-solid turbulent flow into a continuous field and a spatially uncorrelated random distribution: theoretical formalism and numerical study. *J. Fluid Mech.* **533**, 1–46.

FRERET, L., THOMINE, O., LAURENT, F., REVEILLON, J. & MASSOT, M. 2012 On the ability of the Eulerian multi-fluid model to predict preferential segregation and flame dynamics in polydisperse evaporating sprays. *Combustion and Flame (submitted)* .

GIRIMAJI, S. S. 1996 Fully explicit and self-consistent algebraic Reynolds stress model. *Theoretical and Computational Fluid Dynamics* **8** (6), 387–402.

KAH, D., LAURENT, F., FRÉRET, L., DE CHAISEMARTIN, S., FOX, R., REVEILLON, J. & MASSOT, M. 2010 Eulerian quadrature-based moment models for dilute polydisperse evaporating sprays. *Flow, Turbulence and Combustion* **85**, 649–676, 10.1007/s10494-010-9286-z.

KAUFMANN, A., MOREAU, M., SIMONIN, O. & HELIE, J. 2008 Comparison between

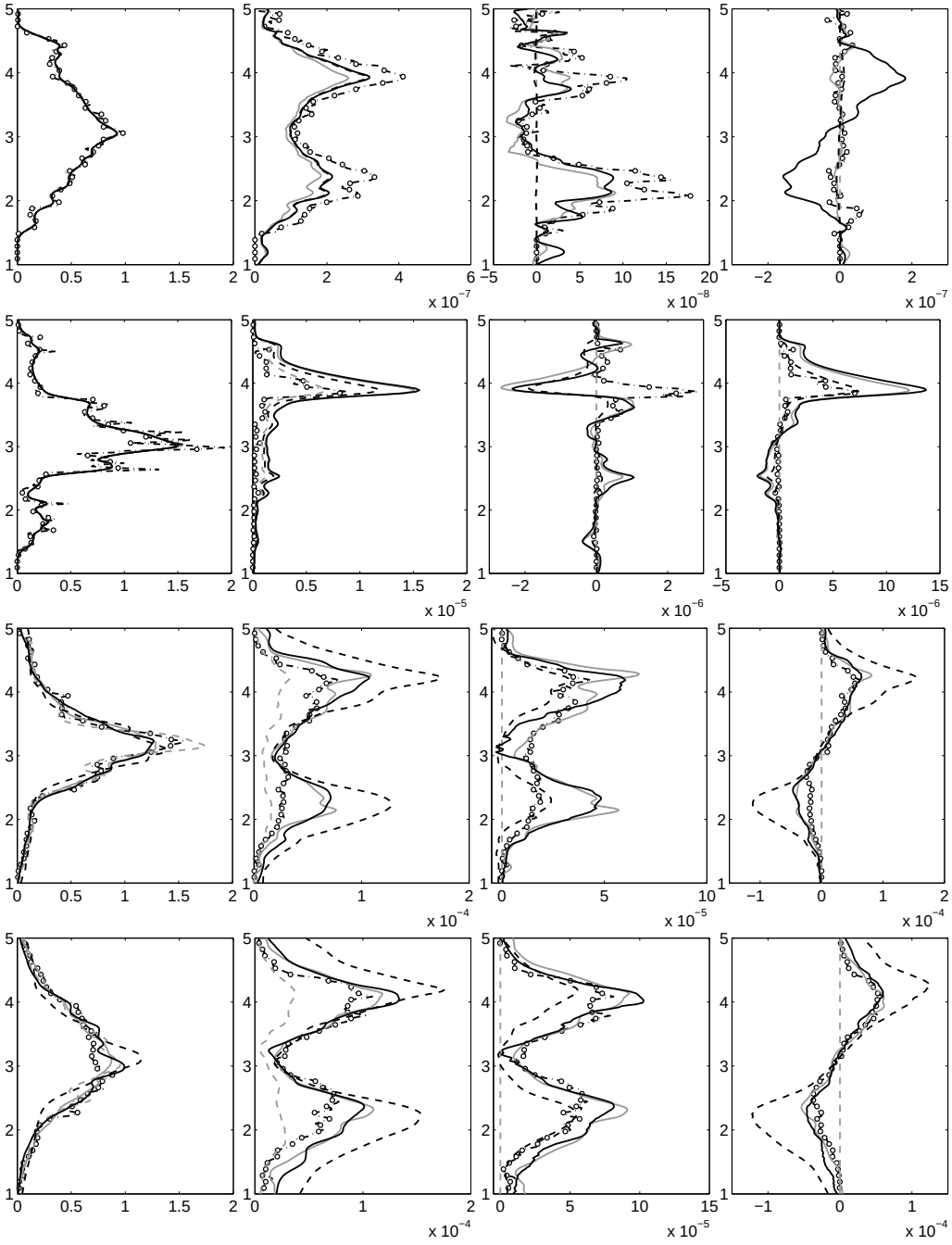

FIGURE 2. Statistics of 256^2 DNS at the time $t = 105s$. From left to right: Mean (over x-direction) profiles of the number density n_p, the RUM kinetic energy $\delta\theta p$ and the deviatoric components of the stress tensor $R^*_{p,11}$ and $R^*_{p,12}$. From top to bottom: St ≈ 0.1, St ≈ 1, St ≈ 5, St ≈ 10. Lagrangian: dot-dashed line with circles, ANISO: full gray line, ISO: dashed gray line, 2Φ-EASM: full black line, VISCO: dashed black line

Lagrangian and mesoscopic Eulerian modelling approaches for inertial particles suspended in decaying isotropic turbulence. *J. Comput. Phys.* **227**, 6448–6472.

Laurent, F. & Massot, M. 2001 Multi-fluid modeling of laminar poly-dispersed spray flames: origin, assumptions and comparison of sectional and sampling methods. *Combust. Theor. Model.* **5**, 537–572.

van Leer, B. 1979 Towards the ultimate conservative difference scheme V. A second order sequel to Godunov's method. *J. Comput. Phys.* **32**, 101–136.

Levermore, C. & Morokoff, W. 1996 The Gaussian moment closure for gas dynamics. *SIAM J. Appl. Math.* **59**, 72–96.

Masi, E. 2010 Theoretical and numerical study of the modeling of unsteady non-isothermal particle-laden turbulent flows by an Eulerian-Eulerian approach. PhD thesis, INP Toulouse.

Masi, E., Riber, E., Sierra, p., Simonin, O. & Gicquel, L. 2010 Modeling the random uncorrelated velocity stress tensors for unsteady particle eulerian simulation in turbulent flows. In *Proceedings of ICMF'10*.

Masi, E. & Simonin, O. 2012 An algebraic-closure-based moment method for unsteady Eulerian modeling of non-isothermal particle-laden turbulent flows in very dilute regime and high Stokes number. *Turb. Heat and Mass Transf.* **7**, 1–12.

Massot, M., Knikker, R., Péra, C. & Reveillon, J. 2004 Lagrangian/Eulerian analysis of the dispersion of evaporating droplets in a non-homogeneous turbulent flow. In *Proceedings of ICMF'04*.

Riber, E. 2007 Développement de la méthode de simulation aux grandes échelles pour les écoulements diphasiques turbulents. PhD thesis, INP Toulouse.

Schumann, U. 1977 Realizability of reynolds-stress turbulence models. *Phys. Fluids* **20** (5), 721–725.

Sierra, P. 2012 Modeling the dispersion and evaporation of sprays in aeronautical combustion chambers. PhD thesis, INP Toulouse.

Simonin, O., Février, P. & Lavieville, J. 2002 On the spatial distribution of heavy particle velocities in turbulent flow: from continuous field to particulate chaos. *J. Turb.* **3(1)**, 40.

So, R., Jin, L. & Gatski, T. 2004 An explicit algebraic stress and heat flux model for incompressible turbulence: Part II Buoyant flow. *Theoret. Comput. Fluid Dynamics* **17** (377406).

Vermorel, O., Bédat, B., Simonin, O. & Poinsot, T. 2003 Numerical study and modelling of turbulence modulation in a particle laden slab flow. *J. Turb.* **335**, 75–109.

Vié, A., Chalons, C., Fox, R. O., Laurent, F. & Massot, M. 2011 A multi-Gaussian quadrature method of moments for simulating high-Stokes-number turbulent two-phase flows. *Annual Research Briefs of the CTR,* pp. 309–320.

Vié, A., Doisneau, F., Laurent, F. & Massot, M. 2012 On the Anisotropic Gaussian closure for the prediction of inertial-particle laden flows. *CICP (submitted)* .

Yuan, C. & Fox, R. 2011 Conditional quadrature method of moments for kinetic equations. *J. Comput. Phys.* **230(22)**, 8216–8246.